Langmuir
Article
pubs.acs.org/Langmuir

High Density Scaffolding of Functional Polymer Brushes: Surface Initiated Atom Transfer Radical Polymerization of Active Esters

Sara V. Orski, Kristen H. Fries, Gareth R. Sheppard, and Jason Locklin*

Department of Chemistry, Faculty of Engineering, and the Center for Nanoscale Science and Engineering, University of Georgia, Athens, Georgia 30602

Received July 13, 2009. Revised Manuscript Received September 8, 2009

In this Article, we describe a method for the polymerization of active esters based on *N*-hydroxysuccinimide 4-vinyl benzoate (NHS4VB) using surface initiated atom transfer radical polymerization (SI-ATRP). Poly(NHS4VB) brushes have high grafting density and a uniform and smooth morphology, and film thickness increases linearly with reaction time. Block copolymer brushes with 2-hydroxyethyl acrylate, *tert*-butyl acrylate, and styrene were synthesized from surface bound poly(NHS4VB) macroinitiators. The active ester brushes show rapid and quantitative conversion under aminolysis conditions with primary amines, which was studied using grazing incidence attenuated total reflection Fourier transform infrared (GATR-FTIR) and UV−vis spectroscopy. UV−vis was also used to quantify the amount of reactive groups in polymer brush layers of differing thickness. Functionalization of the active ester pendant groups with chromophores containing primary amines showed a linear correlation between the amount of chromophore incorporated into the brush layer and brush thickness. Grafting densities as high as 25.7 nmol/cm^2 were observed for a 50 nm brush. Block copolymer brushes with buried active ester functional moieties also undergo quantitative conversion with primary amines as confirmed by GATR-FTIR. We discuss the potential of activated ester brushes as universal scaffolds for sensor and microarray surfaces, where the twofold control of functionalizable active ester polymer and block copolymers provides well-ordered, tunable microenvironments.

Introduction

Using polymer substrates as the immobilization matrix for affinity biosensors and microarrays has enabled advances in biotechnology, medical diagnostics, drug screening, combinatorial chemistry, and many other areas of interest.[1] Signal amplification techniques, such as fluorescence tagging, can effectively detect very small analyte concentrations but can interfere with the native microenvironment, conformation of the molecule, and/or binding kinetics.[2] Specifically, optical biosensors, such as those based on surface plasmon resonance (SPR) have become more commonplace as a real-time, label free technique because no signal amplification of a binding event is necessary.[3] This has led to the determination of both thermodynamic and kinetic parameters for many adsorption/hybridization events between biological species.[4−6]

When designing an immobilization matrix for surface biosensors and microarrays, factors such as the density, activity, orientation, and conformation of immobilized probe molecules influence the activity and effectiveness of the binding event.[7] The matrix must also comply with requirements of minimal nonspecific adsorption and provide stability to environmental changes such as ionic strength, pH, or temperature fluctuations. A degree of specification in the immobilization matrix is necessary for different types of arrays and sensors. A specific example is that surfaces amenable for oligonucleotide arrays are not well suited for use with proteins because of the biophysical and biochemical differences between the two classes of molecules.[8] Ultimately, techniques that afford coatings with easily tunable parameters provide the most versatility.

Many strategies have been employed to attach polymers to a sensing platform as an immobilization matrix. Among these are the formation of self-assembled monolayers (SAMs) consisting of low molecular weight polymer chains,[9] grafting of polymers with predefined molecular weight to a surface through covalent bonding of a SAM with functional groups on the polymer ("grafting to"),[10,11] or by synthesizing polymer brushes from the substrate surface ("grafting from") and derivatizing the pendant groups on the polymer.[12,13] Specifically for SPR substrate chips, carboxymethyl dextrans are often used as a solid support matrix and are commercially available.[14] These carbohydrates are grafted to the surface and derivatized using a sequence of reactions to form activated ester leaving groups along the polymer backbone. These reactive groups facilitate nucleophilic attack with amine terminated moieties and subsequent functionalization of the polymer matrix. Carboxymethyl dextrans and other "grafting to" polymers, used as immobilization matrices, are often hydrophilic to prevent nonspecific adsorption of biological analytes.[15,16]

*Corresponding author. E-mail: jlocklin@chem.uga.edu.

(1) Borisov, S. M.; Wolfbeis, O. S. *Chem. Rev.* **2008**, *108*(2), 423–461.
(2) Haab, B. B. *Proteomics* **2003**, *3*(11), 2116–2122.
(3) Homola, J. *Chem. Rev.* **2008**, *108*(2), 462–493.
(4) Hook, A. L.; Thissen, H.; Voelcker, N. H. *Biomacromolecules* **2009**, *10*(3), 573–579.
(5) Cretich, M.; Pirri, G.; Damin, F.; Solinas, I.; Chiari, M. *Anal. Biochem.* **2004**, *332*(1), 67–74.
(6) Fixe, F.; Dufva, M.; Telleman, P.; Christensen, C. B. V. *Nucleic Acids Res.* **2004**, *32*(1), e9.
(7) Yalçin, A.; Damin, F.; Özkumur, E.; di Carlo, G.; Goldberg, B. B.; Chiari, M.; Unlü, M. S. *Anal. Chem.* **2008**, *81*(2), 625–630.
(8) Kusnezow, W.; Hoheisel, J. D. *J. Mol. Recognit.* **2003**, *16*(4), 165–176.
(9) Ladd, J.; Taylor, A. D.; Pillarik, M.; Homola, J.; Jiang, S. *Anal. Bioanal. Chem.* **2009**, *393*, 1157–1163.
(10) Malmqvist, M.; Karlsson, R. *Curr. Opin. Chem. Biol.* **1997**, *1*, 378–383.
(11) Löfas, S.; Johnsson, B.; Edström, Å.; Hansson, A.; Lindquist, G.; Hillgren, R.-M. M.; Stigh, L. *Biosens. Bioelectron.* **1995**, *10*(9−10), 813–822.
(12) Jain, P.; Dai, J.; Baker, G. L.; Bruening, M. L. *Macromolecules* **2008**, *41* (22), 8413–8417.
(13) Tsujii, Y. O; Yamamoto, S.; Goto, A.; Fukuda, T. *Adv. Polym. Sci.* **2006**, *197*, 1–45.
(14) Biacore Life Sciences Division, http://www.biacore.com/lifesciences/index.html (accessed July **2009**).
(15) Hucknall, A.; Rangarajan, S.; Chilkoti, A. *Adv. Mater.* **2009**, *21*(23), 2441–2446.
(16) Monchaux, E.; Vermette, P. *Langmuir* **2007**, *23*(6), 3290.

This hydrophilicity, along with the cross-links that occur between the polymer chains and the surface (and often between the polymer chains themselves), create a hydrogel matrix that is sensitive to pH and ionic strength of its solution environment.[17] This can create an environmental background response that can complicate or even mask binding events that occur at the substrate interface.

N-Hydroxysuccinimide (NHS) esters are the most common reactive group of activated esters and are widely used to conjugate biological analytes to solid supports in their native form, where the N-terminus of peptides, or lysine side chains, covalently bind at the active ester site.[18] While NHS esters have a half-life on the order of hours in aqueous systems, their rate of hydrolysis increases in basic environments.[18−20] Also, side reactions involving ring-opening or glutarimide formation between two active esters are possible.[21] Functionalization strategies can minimize side reactions in active ester functionalization, such as using a high concentration of the desired amine moiety to be attached or functionalizing in organic solvents in the presence of a proton acceptor such as triethylamine or 4-(dimethylamino)pyridine.[18,22]

More recently, the synthesis of polymers containing active ester groups has emerged as a popular strategy for coupling synthetic and biomacromolecules.[23−31] By polymerizing a monomer with an active ester functionality, not only is the extra functionalization step avoided, but the polymer becomes a template for many types of pendant functional groups and molecules. Pendant group functionalization is straightforward and shows first order reaction kinetics with very fast reaction times.[32] It has been shown that synthetic polymers coupled to proteins can improve the overall protein stability, solubility, and biocompatibility and are being utilized in the fields of biotechnology and medicinal research.[33,34] Controlled polymerizations containing active esters, including the development of block copolymers, have been achieved in solution by controlled polymerization techniques such as atom transfer radical polymerization (ATRP),[35−37] nitroxide mediated polymerization (NMP),[38] ring-opening metathesis polymerization (ROMP),[39−41] and reversible addition−fragmentation chain transfer (RAFT) polymerization.[42−44]

As controlled polymer architectures of active ester polymers have advanced in solution, there are few reports of these polymers grafted from solid interfaces. The Rühe group has polymerized *N*-methacryloyl-β-alanine succinimide ester via a free-radical polymerization from a surface bound 2,2′-azobis(2-methylpropionitrile) (AIBN) initiator and demonstrated the functionalization of the activated ester with small molecules and oligomers on polymer thicknesses up to 80 nm.[45] More recently, Cullen and coworkers used ATRP to grow polymer brushes of 2-vinyl-4, 4-dimethyl azlactone from a surface to immobilize RNase A and showed the enzyme maintained activity while covalently attached to the polymer matrix.[46] In order to fully develop active ester brushes as a versatile and practical template for sensors and microarrays, the stability of the activated ester brushes and the ability to make controlled block copolymer architectures must be evaluated. By polymerizing activated ester monomers using a controlled polymerization technique, the sensing platform has two facets of control. The NHS ester provides the desired attachment chemistry, while the ability to polymerize blocks of different monomers can control the surrounding microenvironment and density of functional groups in the brush. This allows for systematic tuning of properties that are important in array development such as nonspecific binding, polymer solubility, and accessibility of the functional moiety to solution analytes. Herein, we report the surface initiated ATRP of *N*-hydroxysuccinimide 4-vinyl benzoate (NHS4VB). We demonstrate controlled polymerization through a kinetic study and formation of block copolymers with 2-hydroxyethyl acrylate, *tert*-butyl acrylate, and styrene in which the NHS block can be either buried or exposed in the brush layer, depending on monomer sequence in the polymerization. To test and quantify the functionalization efficiency, the poly(NHS4VB) brushes are functionalized with primary amine containing chromophores to quantify the amount of activated ester present in the brush architecture and evaluate the conversion efficiency of amide formation along the chain backbone. The NHS active ester polymer brushes have the potential to serve as a universal scaffold for the attachment of both large and small analytes for sensor and microarray surfaces.

Experimental Section

Materials. All solvents, with the exception of dimethyl sulfoxide (DMSO) and anisole, were distilled from sodium-ketyl (THF) or calcium hydride (toluene and dichloromethane). Anhydrous DMSO and dimethylformamide (DMF) (Drisolv, 99.8% by GC) were purchased from EMD. Anisole was purchased from Alfa Aesar and used as received. Silicon wafers (orientation ⟨100⟩, native oxide) were purchased from University Wafer. BK7 microscope slides (RI = 1.514) were purchased from VWR. *tert*-Butyl acrylate, 2-hydroxyethyl acrylate, and styrene were flashed through a basic alumina column to remove inhibitor. All other chemicals were purchased from Sigma Aldrich and were used as received.

Preparation of Gold Substrates. Microscope slides were cleaned by sonication in isopropyl alcohol for 15 min each. Slides were rinsed with isopropyl alcohol and dried under a stream of argon. Chromium (2 nm) and gold (47 nm) were deposited on the

(17) Xu, F.; Persson, B.; Lofas, S.; Knoll, W. *Langmuir* **2006**, *22*(7), 3352–3357.
(18) Hermanson, G. T.; *Bioconjugate Techniques*, 2nd ed.; Academic Press: New York, 2008.
(19) Lomant, A. J.; Fairbanks, G. *J. Mol. Biol.* **1976**, *104*, 243–261.
(20) Staros, J. V. *Acc. Chem. Res.* **1988**, *21*, 435–441.
(21) Devenish, S. R. A.; Hill, J. B.; Blunt, J. W.; Morris, J. C.; Munro, M. H. G. *Tetrahedron Lett.* **2006**, *47*(17), 2875–2878.
(22) Wong, S. Y.; Putnam, D. *Bioconjugate Chem.* **2007**, *18*(3), 970–982.
(23) Wood, K. C.; Azarin, S. M.; Arap, W.; Pasqualini, R.; Langer, R.; Hammond, P. T. *Bioconjugate Chem.* **2008**, *19*(2), 403–405.
(24) Pasut, G.; Mero, A.; Caboi, F.; Scaramuzza, S.; Sollai, L.; Veronese, F. M. *Bioconjugate Chem.* **2008**, *19*(12), 2427–2431.
(25) Chen, G.; Huynh, D.; Felgner, P. L.; Guan, Z. *J. Am. Chem. Soc.* **2006**, *128* (13), 4298–4302.
(26) Theato, P.; Zentel, R. *Langmuir* **2000**, *16*(4), 1801–1805.
(27) Theato, P. *J. Polym. Sci., Part A: Polym. Chem.* **2008**, *46*(20), 6677–6687.
(28) Hausch, M.; Zentel, R.; Knoll, W. *Macromol. Chem. Phys.* **1999**, *200*(1), 174–179.
(29) Buck, M. E.; Breitbach, A. S.; Belgrade, S. K.; Blackwell, H. E.; Lynn, D. M. *Biomacromolecules* **2009**, *10*(6), 1564–1574.
(30) Buck, M. E.; Zhang, J.; Lynn, D. M. *Adv. Mater.* **2007**, *19*(22), 3951–3955.
(31) Barringer, J. E.; Messman, J. M.; Banaszek, A. L.; Meyer, H. M.; Kilbey, S. M. *Langmuir* **2008**, *25*(1), 262–268.
(32) Eberhardt, M.; Theato, P. *Macromol. Rapid Commun.* **2005**, *26*, 1488–1493.
(33) Heredia, K. L.; Maynard, H. D. *Org. Biomol. Chem.* **2007**, *5*(1), 45–53.
(34) Kiick, K. L. *Science* **2007**, *317*(5842), 1182–1183.
(35) Monge, S.; Haddleton, D. M. *Eur. Polym. J.* **2004**, *40*(1), 37–45.
(36) Pedone, E.; Li, X.; Koseva, N.; Alpar, O.; Brocchini, S. *J. Mater. Chem.* **2003**, *13*, 2825–2837.
(37) Theato, P.; Kim, J.-U.; Lee, J.-C. *Macromolecules* **2004**, *37*(15), 5475–5478.
(38) Desai, A.; Atkinson, N.; Rivera, F. J.; Devonport, W.; Rees, I.; Branz, S. E.; Hawker, C. J. *J. Polym. Sci., Part A: Polym. Chem.* **2000**, *38*(6), 1033–1044.
(39) Strong, L. E.; Kiessling, L. L. *J. Am. Chem. Soc.* **1999**, *121*, 6193–6196.
(40) Vogel, N.; Theato, P. *Macromol. Symp.* **2007**, *249/250*, 383–391.
(41) Carrillo, A.; Yanjarappa, M. J.; Gujraty, K. V.; Kane, R. S. *J. Polym. Sci., Part A: Polym. Chem.* **2006**, *44*(2), 928–939.
(42) Savariar, E. N.; Thayumanavan, S. *J. Polym. Sci., Part A: Polym. Chem.* **2004**, *42*(24), 6340–6345.
(43) Nilles, K.; Theato, P. *Eur. Polym. J.* **2007**, *43*, 2901–2912.
(44) Li, Y.; Lokitz, B. S.; McCormick, C. L. *Macromolecules* **2005**, *39*(1), 81–89.
(45) Murata, H.; Prucker, O.; Rühe, J. *Macromolecules* **2007**, *40*(15), 5497–5503.
(46) Cullen, S. P.; Mandel, I. C.; Gopalan, P. *Langmuir* **2008**, *24*(23), 13701–13709.

glass slides by thermal evaporation (VE-90, Thermionics Northwest). The slides were then transferred immediately to a plasma vapor deposition chamber (PVD-75, Kurt Lesker), where 3.6 nm of silicon oxide was deposited on top of the gold layer.

Preparation of SI-ATRP Initiator Layers. Silicon wafers, SPR substrates, and glass slides were cut into rectangular pieces (approximately 7 × 20 mm^2) and sonicated for 5 min each in acetone, ethanol, and deionized water (18.2 MΩ) water. The wafers were dried under a stream of argon and then subjected to plasma cleaning (Harrick Plasma model PDC-32-G, atmospheric gas, 0.8 mbar, 6.8 W) for 2 min. The initiator, 11-(2-bromo-2-methyl)propionyloxyundecenyl trichlorosilane, was synthesized following literature procedures.[47] The substrates and all dry, degassed reagents were transferred into a nitrogen filled glovebox. One drop of initiator was mixed with 20 mL of dry, degassed toluene (approximate concentration 10 mM), and the solution was filtered through a 0.45 μm poly(tetrafluoroethylene) filter and poured over the clean silicon wafers in a glass staining jar. After 16 h, the substrates were removed, rinsed with freshly distilled toluene, and stored in toluene. The self-assembled monolayer was 2.5 nm, measured by ellipsometry. An atomic force microscopy (AFM) topographic image of the monolayer was featureless, with a rms roughness of 1.2 nm.

Synthesis of *N*-Hydroxysuccinimide 4-Vinyl Benzoate (NHS4VB). NHS4VB was prepared in a three step procedure from 4-bromobenzaldehyde. Briefly, 4-bromobenzaldehyde was converted to 4-bromostyrene using Wittig chemistry with triphenylphosphine methyl ylide.[48] 4-Bromostyrene was converted to 4-vinylbenzoic acid through Grignard formation and quenching with CO_2. Finally, coupling of *N*-hydroxysuccinimide with 4-vinylbenzoic acid gave the active ester NHS4VB.[49,50]

Polymerization of NHS4VB. The initiator substrate and a micro stirbar were placed in a dry, flat bottom Schlenk flask in the glovebox. The NHS4VB monomer (0.662 g, 2.7 mmol) and 0.5 mL of DMSO were added to the Schlenk flask. Separately, a stock solution was made that consisted of 0.5 mL of DMSO, *N*,*N*,*N*′,*N*″,*N*‴-pentamethyldiethylenetriamine (PMDETA, 423 μL, 2.03 mmol), copper(I) bromide (39 mg, 0.27 mmol), and copper(II) chloride (7.26 mg, 0.05 mmol). An aliquot of 93 μL of the stock solution was added to the Schlenk flask, which was then sealed, brought outside the glovebox, and stirred in a 50 °C oil bath for 16 h. The flask was then opened and exposed to air, and the wafers were rinsed vigorously with DMF and dried under a stream of argon.

Determination of the Polymerization Kinetics for NHS4VB. Six identical polymerizations were assembled as described above, using both silicon wafers and glass slides functionalized with initiator. Polymerization was stopped at different time intervals by removing the flask from the oil bath and opening it to air. The substrates were rinsed thoroughly with DMF and dried under argon. Film thicknesses were characterized for polymerization reactions at 15, 30, 45, 60, 120, and 255 min.

Synthesis of Poly(NHS4VB-*b*-HEA) Brushes. The poly(NHS4VB) wafer and a micro stirbar were placed in a dry, flat bottom Schlenk flask in the glovebox. 2-Hydroxyethyl acrylate (0.314 g, 2.7 mmol) and 235 μL of DMSO were added to the Schlenk flask. Separately, a stock solution was made consisting of 0.5 mL of DMSO, PMDETA (423 μL, 2.03 mmol), copper(I) bromide (39 mg, 0.27 mmol), and copper(II) chloride (7.26 mg, 0.05 mmol). A total of 93 μL of the stock solution was added to the Schlenk flask, which was then sealed, brought outside the glovebox, and stirred in a 50 °C oil bath for 16 h.

Synthesis of Poly(NHS4VB-*b*-*t*BA) Brushes. Similar procedure as above. *tert*-Butyl acrylate (0.346 g, 2.7 mmol) and 265 μL of DMSO were added to the Schlenk flask, along with 93 μL of the stock solution to maintain a monomer concentration of 50 wt %. The reaction was stirred in a 50 °C oil bath for 16 h.

Synthesis of Poly(NHS4VB-*b*-styrene) Brushes. Similar procedure as above. Styrene (0.281 g, 2.7 mmol) and 205 μL of DMSO were added to the Schlenk flask, along with 93 μL of the stock solution to maintain monomer concentration of 50 wt %. The reaction stirred in a 50 °C oil bath for 16 h.

Synthesis of Poly(styrene-*b*-NHS4VB) Brushes. To an initiator functionalized silicon wafer in a Schlenk flask, styrene (2.89 g, 27.75 mmol), copper(I) bromide (0.027 g, 0.185 mmol), copper(II) chloride (5 mg, 0.037 mmol), and 2 mL of anisole were added. The flask was bubbled with argon gas for 1 h to purge the system of oxygen, and then PMDETA (291 μL, 1.40 mmol), which was also purged with argon separately, was added to the reaction. The flask was sealed and put in a 90 °C oil bath for 16 h. The substrate was rinsed thoroughly with anisole, dried under argon, and then polymerized with NHS4VB as described above.

Functionalization of Poly(NHS4VB) Brushes with Primary Amines. Polymer brushes, both the polyNHS4VB and relative block copolymer brushes, were converted to functionalized amide derivatives of 4-vinyl benzoic acid using 1-aminomethylpyrene (Py-N) and octadecylamine as model compounds (0.12 M in dry DMF) at 40 °C with triethylamine as a proton acceptor.[45] The glass slides from the polymerization kinetics experiment were functionalized with Py-N and used to quantify the density of functional groups for a given film thickness. Substrates were functionalized with Py-N and removed from the reaction at various times for UV−vis spectroscopy to determine functionalization time for quantitative aminolysis.

Quantification of Active Ester Moiety. The Py-N functionalized glass slides were measured on a UV−vis spectrometer using a slide holder accessory with a sample window area of 19.6 mm^2. A calibration curve using Py-N in DMF solution was created with concentrations between 5.0×10^{-6} and 3.3×10^{-5} M. The rate of substitution of Py-N onto the polymer brush was measured by monitoring the appearance of Py-N absorbance with time by UV−vis spectroscopy.

Characterization. Ellipsometry, static contact angle measurements, and surface plasmon resonance were all performed on a Multiskop (Optrel GbR) instrument. Null ellipsometry was performed using a HeNe laser at $\lambda = 632.8$ nm at 70°, and film thicknesses were determined using integrated specific software. At least three spots on each wafer were measured, and the thickness was averaged. To obtain thickness values of the samples, a simple box model was employed and a refractive index of $n = 1.50$ was assumed for all polymer brush layers. SPR measurements were taken in the Kretchmann configuration. Atomic force microscopy images were taken using tapping mode on a Multimode NanoScope IIIa (Digital Instruments/Veeco Metrology) instrument using silicon AFM probes with a 300 kHz resonant frequency and a 40 N/m spring constant. UV−vis spectroscopy was taken on a Varian 50Bio spectrometer. Fourier transform infrared (FTIR) measurements were taken with a Nicolet model 6700 instrument with a grazing angle attenuated total reflection accessory (GATR) at 256 scans with 4 cm^{-1} resolution.

Results and Discussion

Synthesis of Active Ester Polymer Brushes. In our initial studies of surface initiated polymerization with active esters, we explored methacrylate-based monomers, such as *N*-hydroxysuccinimidyl methacrylate (NHSMA), as this monomer has been polymerized by ATRP in solution. When attempting surface initiated polymerization, despite changing reaction temperature

(47) Matyjaszewski, K.; Miller, P. J.; Shukla, N.; Immaraporn, B.; Gelman, A.; Luokala, B. B.; Siclovan, T. M.; Kickelbick, G.; Vallant, T.; Hoffmann, H.; Pakula, T. *Macromolecules* **1999**, *32*(26), 8716–8724.
(48) Nozaki, K.; Sato, N.; Tonomura, Y.; Yasutomi, M.; Takaya, H.; Hiyama, T.; Matsubara, T.; Koga, N. *J. Am. Chem. Soc.* **1997**, *119*(52), 12779–12795.
(49) Angiolini, L.; Caretti, D.; Mazzocchetti, L.; Salatelli, E.; Willem, R.; Biesemans, M. *J. Organomet. Chem.* **2006**, *691*(13), 3043–3052.
(50) Aamer, K. A.; Tew, G. N. *J. Polym. Sci., Part A: Polym. Chem.* **2007**, *45*, 5618–5625.

Scheme 1. Scheme of SI-ATRP of NHS4VB with Twofold Control of Polymer Architecture[a]

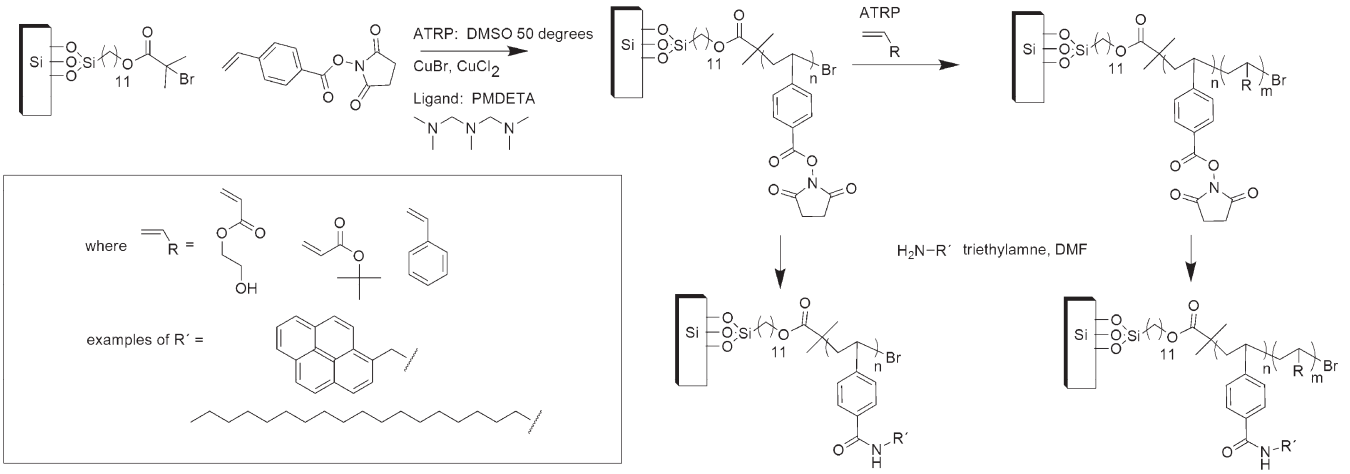

[a] Poly(NHS4VB) can act as a macroinitiator to form block copolymers with a variety of monomers with subsequent derivatization of the NHS containing block.

and solvent, ratios of Cu(I) and Cu(II), adding sacrificial initiator, and changing monomer concentration, thicknesses greater than 5 nm were not achievable with this monomer. The grazing angle attenuated total reflection spectroscopy (GATR-FTIR) spectrum of poly(NHSMA) brushes showed a significant amount of carboxylic acid present and very little of activated ester. The reason for the reduced film thickness is not completely clear, since the same monomer can be polymerized in a controlled fashion using ATRP in solution, albeit with relatively low molecular weights, less than 50 000 g/mol.[51] Either partial hydrolysis or catalyst deactivation by complexation with the growing polymer chains is a possible reason for early termination. This has been observed with acrylamides and azlactone polymerizations in solution.[52,53] For this reason, we turned to the polymerization of 4-vinyl benzoate derivatives, which are known to polymerize with high reaction rates.[54]

The reaction scheme for the polymerization of NHS4VB and subsequent functionalization can be seen in Scheme 1, which depicts a polymer brush matrix with twofold functionality. First, block copolymers allow for precise spatial placement of functional groups within the brush layer, which can be laterally extended with a block containing different chemical functionality to control the polymer microenvironment. The second dimension of control is the ability to attach new functionality to the polymer brush through conjugation with a primary amine. This allows postfunctionalization of the brush surface with a wide variety of molecules that contain a functionality incompatible with surface polymerization reactions.

A 16 h polymerization (50 wt % in DMSO at 50 °C) yields films with an average thickness of 50 nm. Without the use of a deactivator (copper(II) chloride) in the polymerization mixture, the polymer films generated by SI-ATRP had a rougher surface morphology, with a rms roughness of 2 nm on average, resulting from a faster, less controlled rate of polymerization. Early termination is more prevalent due to the larger concentration of propagating radicals. These radicals, in close proximity to each other, can couple or disproportionate prematurely and cease the polymerization. Polymerization with copper(II) chloride afforded better control; halogen exchange of the alkyl bromide initiator with $CuCl_2$ provides for faster initiation relative to the rate of propagation.[55] The copper(II) also lowers the equilibrium concentration of propagating radicals, which slows propagation and affords better polymer rate control. This resulted in homogeneous film thickness, with deviations of less than 1 nm and an overall uniform, smooth morphology. AFM images of the poly(NHS4VB) brushes prepared with and without Cu(II) are shown in Figure 1. In the polymerization with $CuCl_2$ added to the reaction mixture, the overall brush morphology is featureless with a rms roughness of 0.5 nm on silicon oxide and 1.5 nm on the gold/silicon oxide surface, which is comparable to the rms roughness of the substrates themselves.

Chemical functionality of the initiator layer, polymer brush, and derivitized polymer substrate was confirmed by GATR-FTIR. Figure 2 shows the stepwise chemical processes required to convert a surface into a reactive ester scaffold. Figure 2a verifies the surface attachment of the initiator, 11-(2-bromo-2-methyl)-propionyloxyundecenyl trichlorosilane, shown by the methyl stretch at 2963 cm^{-1} and the carbonyl stretch at 1737 cm^{-1}. The spectra of the polymer brush can be seen in Figure 2b. The peaks at 1801, 1769, and 1738 cm^{-1} are carbonyl stretches of the NHS activated ester derivative, while the C−O stretches are visible at 1258 and 1026 cm^{-1}. The peak at 1258 cm^{-1} is due to the C−N stretch of NHS. Poly(NHS4VB) was then functionalized with aminomethylpyrene (Py-N), indicated by the amide I and II stretches at 1642 and 1542 cm^{-1}, respectively (Figure 2c). A thorough assignment of the vibrations in the initiator and surface bound polymer brushes is highlighted in Table 1 of the Supporting Information.

In order to utilize the surface bound active ester chains for SPR analysis, the initiator layer must be stable to elevated reaction temperatures, dependent on the conditions for copolymerization and the type of monomer used. This presents a limitation on using a noble metal surface as an SPR platform, due to the thermal lability of the metal−thiol bond used to anchor the initiator layer. Depositing a thin layer of silicon oxide (~4 nm) on top of the metal substrate can circumvent this problem. By utilizing silane chemistry to anchor the initiator species, the SAM is much more

(51) Godwin, A.; Hartensteing, M.; Muller, A. H. E.; Brocchini, S. *Angew. Chem., Int. Ed.* **2001**, *40*(3), 594–587.
(52) Teodorescu, M.; Matyjaszewski, K. *Macromolecules* **1999**, *32*(15), 4826–4831.
(53) Fournier, D.; Pascual, S.; Fontaine, L. *Macromolecules* **2004**, *37*(2), 330–335.
(54) Matyjaszewski, K.; Davis, T. P. *Handbook of Radical Polymerization*; John Wiley and Sons, Inc.: Hoboken, NJ, 2002; p 534.
(55) Matyjaszewski, K.; Shipp, D. A.; Wang, J.-L.; Grimaud, T.; Patten, T. E. *Macromolecules* **1998**, *31*(20), 6836–6840.

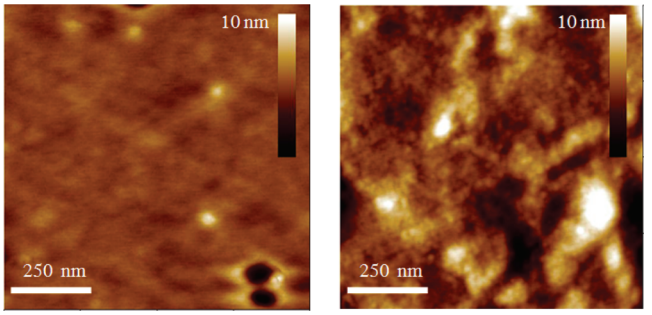

Figure 1. AFM topography images (1 × 1 μm^2) of 20 nm poly(NHS4VB) brushes polymerized with (left) and without (right) $CuCl_2$.

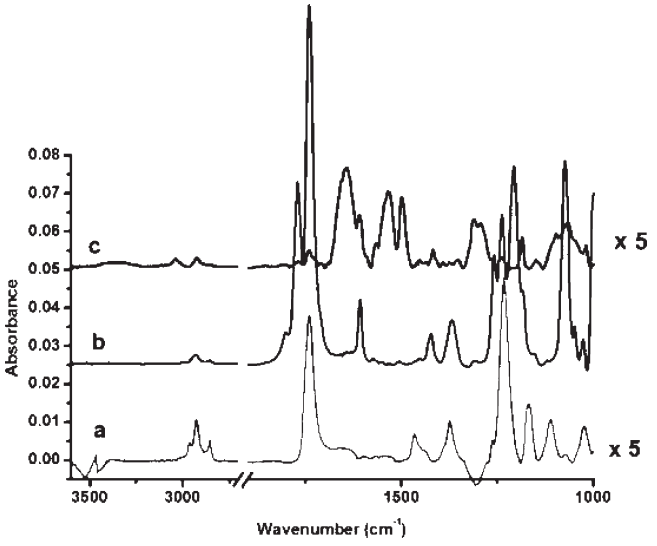

Figure 2. GATR-FTIR of the (a) ATRP initiator, (b) poly(NHS4VB) brush, and (c) poly(NHS4VB) brush functionalized with Py-N.

tolerant to higher temperatures than the thiol anchor group. We have also found that the gold/silicon oxide substrates are robust for polymerization conditions and do not degrade over time. For example, test substrates of gold/silicon oxide were sonicated for 45 min each in dichloromethane, acetone, and water with no degradation or shift in the plasmon resonance angle. For these reasons, poly(NHS4VB) was polymerized on a gold/silicon oxide surface (see the Supporting Information), with times and thicknesses identical to those for polymerization from silicon wafers under the same conditions.

The polymer brush is stable to atmospheric conditions over several months, as poly(NHS4VB) substrates, stored in a Petri dish on the benchtop, were repeatedly measured using contact angle measurements over a period of 120 days. Figure 3 shows the variation in contact angle of the active ester brushes with time. The initial static contact angle of the poly(NHS4VB) was 75° ± 3° and did not decrease with time, indicating the NHS functionality of the film is preserved and does not hydrolyze when stored in ambient conditions. GATR-FTIR spectra taken after 4 months of storage in ambient conditions also confirmed the stability, as there was no change in the absorbance intensity of the characteristic NHS peaks in the spectrum. For comparison, poly(NHS4VB) layers hydrolyzed in aqueous base (50% v/v 0.1 M NaOH and THF) had a contact angle of 34.4°.

Kinetics of Polymerization. Figure 4 shows the increase in film thickness with time as measured by ellipsometry. The polymer brush thickness increases linearly with time for the first

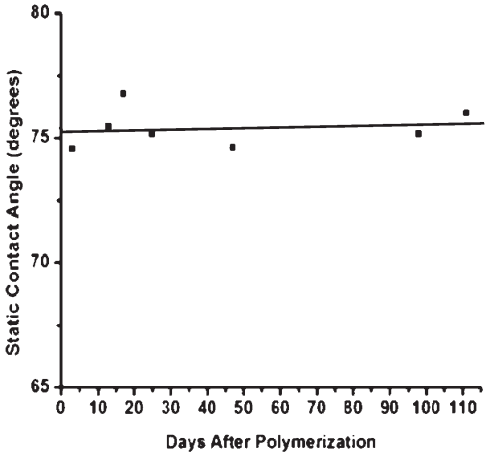

Figure 3. Time-dependent contact angle measurements of the active ester polymer brushes. The stability test was measured over a period of 120 days.

hour in DMSO at 50 °C before plateauing around a thickness of 50 nm. This plateau region, due to early termination reactions, is consistent with other monomers synthesized using SI-ATRP.[12,56] The concentration of propagating radicals on the tethered chains decreases as the chain ends extend, where the close proximity of radicals cause coupling and disproportionation reactions of the radical chain ends.[57]

Block Copolymerizations with Active Ester Polymer Brushes. With the retention of the bromine end group, the poly(NHS4VB) can be chain extended and the controlled nature of SI-ATRP verified. Block copolymers were synthesized using various monomers to explore different backbone functionality and, ultimately, tunable microenvironments. Poly(NHS4VB), with a thickness of 25 nm, was used as a macroinitiator for polymerization of 2-hydroxyethylacrylate (HEA). The thickness of the HEA block was 24 nm after 16 h of polymerization at 50 °C. The GATR-FTIR of the poly(NHS4VB-*b*-HEA) film is shown in Figure 5a. The spectrum shows a combination of vibrations for both NHS4VB and HEA. Specifically, the HEA block is distinguished by the OH stretch and deformation at 3372 and 1396 cm^{-1}, respectively. The ester in the HEA backbone can be identified by the C═O stretch at 1731 cm^{-1} and a C—O stretch at 1175 cm^{-1}. A more thorough peak assignment is shown in Table 1 of the Supporting Information.

tert-Butyl acrylate (*t*BA) was also polymerized from a surface bound poly(NHS4VB) brush macroinitiator. In the block copolymer with *t*BA (Figure 5b), the peaks at 2975 and 1367 cm^{-1} are consistent with the asymmetric stretch and deformation of the CH_3 in the *tert*-butyl group of the second block. In addition, the C═O stretch of the ester observed at 1727 cm^{-1} is due to both the *t*BA and NHS4VB polymer segments. When a thicker macroinitiator layer was used (poly(NHS4VB) = 50 nm), the thickness of the tBA block was 8.3 nm under the same polymerization conditions. The thinner *t*BA layer is probably due to the lack of macroinitiator sites because of early termination reactions in the thicker poly(NHS4VB) film.

Block copolymerization with styrene was achieved using a similar 25 nm poly(NHS4VB) macroinitiator. The thickness of the styrene block was 25 nm after 16 h of polymerization at 90 °C. Since both the NHS4VB and second block are styrene based,

(56) Raynor, J. E.; Petrie, T. A.; Fears, K. P.; Latour, R. A.; García, A. J.; Collard, D. M. *Biomacromolecules* **2009**, *10*(4), 748–755.
(57) Kim, J.-B.; Huang, W.; Miller, M. D.; Baker, G. L.; Bruening, M. L. *J. Polym. Sci., Part A: Polym. Chem.* **2003**, *41*(3), 386–394.

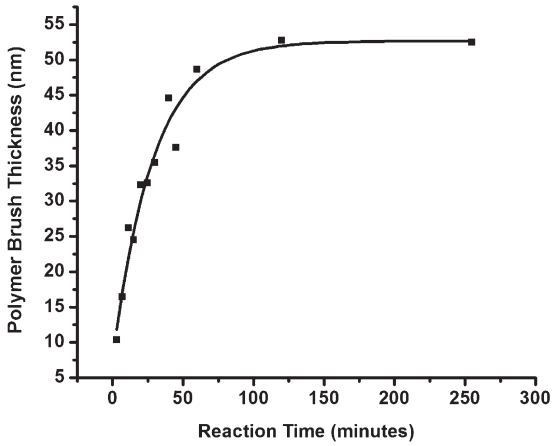

Figure 4. Kinetic curve for the poly(NHS4VB) brushes. Brush thickness increases linearly with reaction time up to 50 nm. The line is meant to guide the eye.

most of the differences in FTIR spectra between the individual polymer and the block copolymer brush (Figure 5c) are relative intensity increases of the aromatic stretching bands with respect to the poly(NHS4VB) alone (Figure 5e). The aromatic C−H stretch at 3000 cm^{-1} is much more prevalent in the block copolymer relative to the C−H stretches of the methylene peaks at 2924 cm^{-1}. This is also true for the ring stretch at 1605 cm^{-1}, where the peak not only increases in intensity relative to the alkyl region but also broadens, due to the slight difference in energy between styrene and the *para*-substituted styrene of the activated ester polymer.

It is interesting to note, when comparing the FTIR spectra of all three block copolymers to the original active ester brush (Figure 5e), the intensities of the characteristic active ester bands, especially those between 1738 and 1801 cm^{-1}, are somewhat diminished and two new bands appear around 1550 and 1450 cm^{-1}. These peaks are assigned to the asymmetric and symmetric stretches of a carboxylate group and denote partial hydrolysis of the active ester during polymerization. Despite exhaustive purification, distillation, and removal of water from the starting materials and polymerization glassware, some loss of the NHS ester does occur in block copolymerization, even though the NHS4VB polymer is stable stored in atmospheric conditions. Because of this reason, we investigated the polymerization of NHS4VB from a surface bound styrene macroinitiator. As can be seen from the retention of the C=O stretches at 1802, 1771, and 1740 cm^{-1} in Figure 5d, no degradation of the brush occurs when NHS4VB is polymerized as the second block. These results are somewhat unexpected, since the reaction conditions for the second block are identical to those for the first, with the only difference being the incorporation of a new monomer into the reaction mixture. If conditions were favorable to cause hydrolysis of the ester, then this loss of the NHS ester would be observed for the poly(NHS4VB) brush as well. This, however, does not negate the efficacy of using ATRP for controlled block copolymer synthesis for complex active ester polymer architectures. The poly(NHS4VB-*b*-styrene) can be regenerated in a solution of EDC/NHS, and the FTIR spectrum (Figure 6a) shows the appearance of the active ester peaks, the disappearance of COO^- stretches at 1550 and 1450 cm^{-1}, and the enhancement of the aromatic ring and C−H stretches. This brush was then functionalized with octadecylamine (ODA) to show that the NHS ester retains its activity toward nucleophilic substitution with primary amines (Figure 6b). The complete conversion of NHS ester with

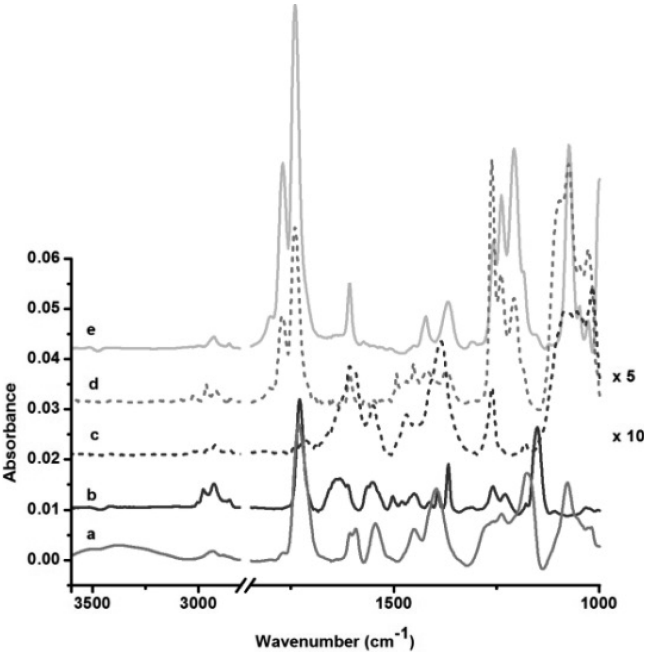

Figure 5. FTIR spectra of block copolymers grown from poly(NHS4VB): (a) poly(NHS4VB-*b*-HEA), (b) poly(NHS4VB-*b*-tBA), (c) poly(NHS4VB-*b*-styrene), (d) poly(styrene-*b*-NHS4VB), and (e) original poly(NHS4VB) for comparison.

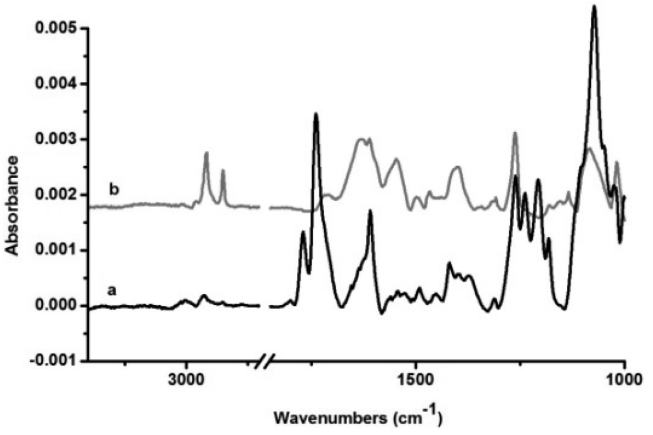

Figure 6. FTIR spectra of block copolymers of poly(NHS4VB-*b*-styrene). (a) The EDC/NHS regenerated active ester block copolymer brush of poly(NHS4VB-*b*-styrene) reacts quantitatively with octadecyl amine (b).

ODA, as seen in the formation of the amide I and II stretches at 1542 and 1532 cm^{-1} and the methyl stretch at 2975 cm^{-1}, indicates that the second block does not prevent adequate diffusion of the analyte into the functional polymer brush.

Aminolysis of the Active Ester Brushes. Poly(NHS4VB) brushes were reacted with 1-aminomethylpyrene (Py-N) or octadecylamine (ODA) to quantify both the kinetic and degree of conversion with primary amines. The poly(NHS4VB) polymer brushes, which had an initial contact angle of 75°, were functionalized with Py-N or ODA to give final contact angles of 93.5° and 94.2°, respectively. FTIR spectra taken after functionalization indicate quantitative conversion of the active ester to amide. When comparing the original poly(NHS4VB) films (Figure 2b) with a brush functionalized with Py-N (Figure 2c), one can see the almost complete disappearance of the imide ring stretches at 1801 and 1769 cm^{-1} and the ester carbonyl and carbon/oxygen

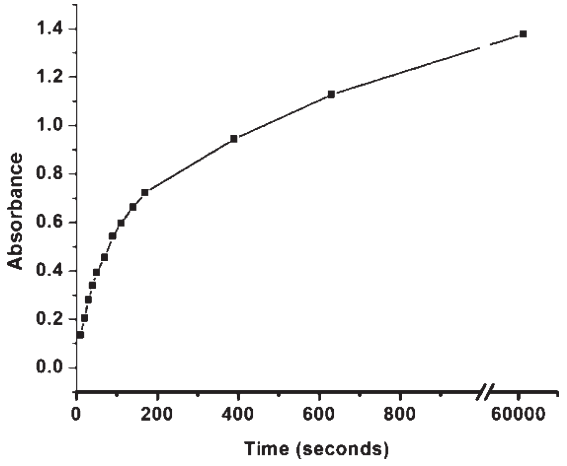

Figure 7. Time-dependent functionalization of poly(NHS4VB) with Py-N. The absorbance maximum of Py-N in the brush occurs at 351 nm.

stretches at 1738, 1258, and 1026 cm^{-1}, while the amide I and amide II bands appear at 1642 and 1542 cm^{-1}. This indicates nearly complete conversion of active ester to amide throughout the 50 nm polymer brush.

Time-dependent UV−vis data was taken to monitor the kinetics of conversion with 1-aminomethylpyrene. A poly(NHS4VB) brush was subjected to aminolysis conditions (0.12 M Py-N in DMF at 40 °C with triethylamine catalyst), and UV−vis absorbance spectra were recorded at different time intervals. Figure 7 plots the absorbance maxima of Py-N (351 nm) with respect to time. The immediate increase in absorbance suggests rapid conversion from the active ester to the amide. The reaction reaches 70% conversion after 6.5 min at 40 °C and reaches maximum conversion overnight.

Quantitative Determination of Available Activated Esters. The relationship between thickness and amount of functionalization was also investigated using UV−vis spectroscopy. Further reactions with 1-aminomethylpyrene were carried out on poly(NHS4VB) brushes grown on glass slides to quantify the number of activated esters in a given area for different brush thicknesses. Separate brush layers of varying thicknesses were subjected to aminolysis with Py-N, and the absorbance values measured by UV−vis spectroscopy. It was assumed the Py-N dye reacts with the NHS ester in a 1:1 molar ratio. The extinction coefficient for Py-N was 32 204 cm^{-1} M^{-1} at 345 nm, measured by a calibration curve in DMF to ensure adequate solvation of the Py-N. Using the Beer−Lambert Law, $A = \varepsilon lc$, one can calculate the surface coverage, $d_{surf} = A\varepsilon^{-1}$.[58] A is absorbance, and ε, l, and c are the extinction coefficient, the thickness of the film, and the concentration of Py-N within the film, respectively. This calculation includes the assumption that the difference in extinction coefficient between Py-N in solution and Py-N in the polymer film is negligible. The linear relationship between polymer brush thickness and NHS concentration is shown in Figure 8. The linear fit shown in the plot has a R^2 value of 0.90 with a standard deviation of 3.2 nmol/cm^2.

The absence of a plateau indicates that substitution occurs throughout the brush matrix and is independent of film thickness. The correlation illustrates the effective diffusion and substitution of Py-N along the entire polymer brush chain, given the complete linear functionalization for the thicknesses studied.

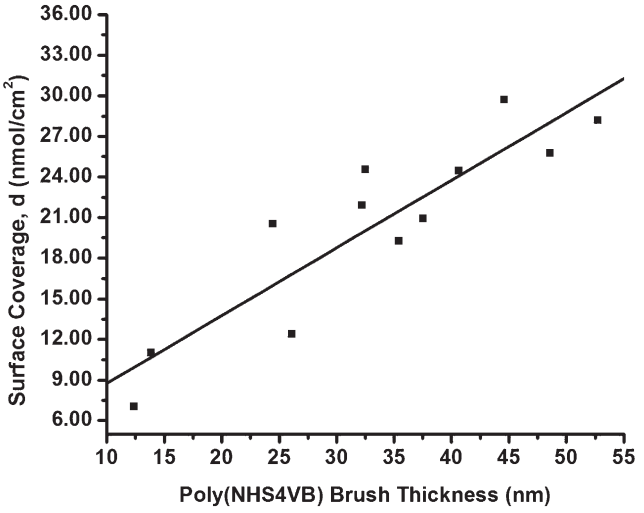

Figure 8. Surface coverage of Py-N on poly(NHS4VB) with increasing film thickness.

Upon functionalization with Py-N, the thickness of the polymer brush layer increases due to the increasing molecular mass of the substituent on the attached polymer molecules. The relationship between thickness change and molecular mass in functional polymer brushes has been studied recently by Rühe et al.[45] If it is assumed that the grafting density of polymer chains before and after functionalization remains constant, the relationship between film thickness and molar masses can be expressed as

$$\frac{L_2}{L_1} = \frac{M_2\rho_1}{M_1\rho_2} \quad (1)$$

where L is the polymer brush thickness, and M and ρ are the molar mass and density of the repeat unit, respectively. The subscripts denote the original (1) and functionalized (2) polymer brush. Since the densities of both polymers are unknown, they can be estimated based on van der Waals radii of molecular fragments as outlined by van Krevelen.[59] The ratio of film thickness of the functionalized and original brush (L_2/L_1 = 1.70) correlates well with the theoretical value (1.62, see the Supporting Information). Since the experimental ratio is approximately equal to (and slightly greater than) the theoretical value, this further indicates near-quantitative conversion of reactive esters with Py-N.

The quantitative functionalization of the brush, along with the linear trend, also provides for a tunable concentration of active ester functionality. Using ATRP, polymer thickness (and thus the number of activated esters in the polymer brush) can be tuned with monomer concentration and reaction time. This technique allows for surfaces with a precisely controlled number of active ester sites within a given area. From the UV−vis experiment, a 50 nm poly(NHS4VB) film can be derivatized with 25.7 nmol/cm^2 Py-N. This is a nearly 3 orders of magnitude improvement in amount of functional sites compared to the case of SAMs with activated ester end groups.[60,61] Thus far, the number of reactive sites in these polymer brushes far outnumbers analyte binding sites in other macromolecular systems. Xu and coworkers determined that the surface coverage of carboxyl groups

(58) Li, D.; Swanson, B. I.; Robinson, J. M.; Hoffbauer, M. A. *J. Am. Chem. Soc.* **1993**, *115*(15), 6975–6980.

(59) van Krevelen, D. W. *Properties of Polymers: Their Estimation and Correlation with Chemical Structure*, 2nd ed.; Elsevier Scientific Publishing: New York, 1976.

(60) Lockett, M. R.; Phillips, M. F.; Jarecki, J. L.; Peelen, D.; Smith, L. M. *Langmuir* **2007**, *24*(1), 69–75.

(61) Gooding, J. J.; Hibbert, D. B. *TrAC, Trends Anal. Chem.* **1999**, *18*(8), 525–533.

in a non-cross-linked carboxymethyl dextran surface was 1.17 nmol/cm^2, which, assuming quantitative functionalization of the NHS ester, is the number of total functional sites in the polymer matrix.[17] Poly(methacrylic acid) polymer brushes were previously activated and derivitized by the Metters group with NHS and then the amino acid trimer of arginine, glyceine, and aspartic acid (RGD) with a molecular weight of 382 g/mol. The measurement of RGD bound within the upper 10 nm of the film was determined to be 8.3 nmol/cm^2.[62] Controlled polymerization with NHS4VB allows not only for a greater number of active binding sites, but also controlled polymer architectures for diffusion of solution analytes to interact along the entire length of the polymer brush backbone.

Conclusions

In summary, we have demonstrated the surface initiated atom transfer radical polymerization of a styrenic-based active ester along with block copolymerization capability. Films of poly(NHS4VB) show a linear increase in film thickness with fast reaction times and can be easily reinitiated to form block copolymers with different types of monomers. This versatility leads to different surface architectures, which depend on the comonomer and functional group coupled to the active ester block. The brushes generated have a uniform, smooth morphology with a high grafting density. Also, postfunctionalization of the NHS4VB moiety shows rapid and quantitative conversion, independent of brush thickness, with small molecule amines. The controlled surface initiated polymerization of active ester polymer brushes and block copolymers will aid in the development of optical sensors and microarrays. With block copolymers, the twofold control over functionality and polymer microenvironment can template many varieties of macromolecular sensing surfaces that may not be easily polymerized from a functional monomer.

Acknowledgment. The authors gratefully acknowledge financial support from the National Science Foundation (ECCS 0901141) and a Faculty of Infectious Diseases seed grant from the University of Georgia Research Foundation, Inc.

Supporting Information Available: Tables of FTIR assignments, surface plasmon resonance analysis of polymer brushes, calculations of molar volume, and assessment of thickness changes for functionalized brushes. This material is available free of charge via the Internet at http://pubs.acs.org.

(62) Harris, B. P.; Kutty, J. K.; Fritz, E. W.; Webb, C. K.; Burg, K. J. L.; Metters, A. T. *Langmuir* **2006**, *22*(10), 4467–4471.